[9] W. A. Edson, *Vacuum Tube Oscillators*. New York: Wiley, 1953, pp. 430–450.
[10] K. Kurokawa, "Some basic characteristics of broad band negative resistance oscillator circuits," *Bell Systems Tech. J.*, pp. 1937–1955, July–Aug. 1969.
[11] W. C. Tsai, F. J. Rosenbaum, and L. A. MacKenzie, "Circuit analysis of waveguide cavity Gunn-effect oscillator," *IEEE Trans. Microwave Theory Tech.*, vol. MTT-18, pp. 808–817, Nov. 1970.
[12] C. P. Jethwa and R. L. Gunshor, "An analytical equivalent circuit representation for waveguide-mounted Gunn oscillators," *IEEE Trans. Microwave Theory Tech.*, vol. MTT-20, pp. 565–572, Sept. 1972.
[13] A. S. Templin and R. L. Gunshor, "Analytical model for varactor-tuned waveguide Gunn oscillators," *IEEE Trans. Microwave Theory Tech.*, vol. MTT-22, pp. 554–556, May 1974.
[14] B. C. Taylor, S. J. Fray, and S. E. Gibbs, "Frequency saturation effects in transferred electron oscillators," *IEEE Trans. Microwave Theory Tech.*, vol. MTT-18, pp. 799–807, Nov. 1970.
[15] W. J. Getsinger, "The packaged and mounted diode as a microwave circuit," *IEEE Trans. Microwave Theory Tech.*, vol. MTT-14, pp. 58–69, Feb. 1966.
[16] R. P. Owens and D. Cawsey, "Microwave equivalent circuit parameters of Gunn-effect-device packages," *IEEE Trans. Microwave Theory Tech.*, vol. MTT-18, pp. 790–798, Nov. 1970.
[17] R. P. Owens, "Mount-independent equivalent circuit of the S4 diode package," *Electronics Letters*, vol. 19, pp. 580–582, Sept. 23, 1971.

Integrated Approach to Microwave Design

JOHN W. BANDLER, SENIOR MEMBER, IEEE, PETER C. LIU, MEMBER, IEEE, AND HERMAN TROMP

Abstract—**A new, integrated approach to microwave design is presented involving concepts such as optimal design centering, optimal design tolerancing, optimal design tuning, parasitic effects, uncertainties in models and reference planes, and mismatched terminations. The approach is of the worst case type, and previously published design schemes fall out as particular cases of the ideas presented. The mathematical and computational complexity as well as the benefits realized by our approach is illustrated by transformer examples, including a realistic stripline circuit.**

I. Introduction

THE use of nonlinear programming techniques for the design of microwave circuits has been well established. Applications hitherto reported by the authors, for example, fall into two categories. 1) The improvement of a response in the presence of parasitics [1], [2], in which case the function to be minimized is of the error function type and the constraints, if any, are normally imposed on the design parameters. 2) Design centering and tolerance assignment to yield a minimum cost circuit that satisfies certain specifications, usually imposed on the frequency response, for all possible values of the actual parameters [3]. The function to be minimized is of the cost function type and the constraints are due to the specifications. Tuning elements may be introduced to further increase possible unrealistic tolerances and thus decrease the cost or make a circuit meet specifications [4].

No consideration, however, of optimal tolerancing or tuning of microwave circuits has been reported where parasitic effects were taken into account. A major complication is introduced here, since the models available for common parasitic elements normally include uncertainties on the value of the model parameters. These uncertainties are due to the fact that the model is usually only approximate and that approximations have to be made in the implementation of existing model formulas. A typical example of the latter is the relationship between the characteristic impedance and width of a symmetric stripline, where the formula involves elliptic integrals.

The model uncertainties can well be of the same order of magnitude as the tolerances on the physical network parameters so that a realistic design, including tolerances, can only be found when allowance is made for them. In the approach adopted, an attempt is made to deal with the model uncertainties in the same way as with the other tolerances. This involves, however, a complication in the formulation of the problem. The physical tolerances affect the physical parameters, whereas the model parameter uncertainties affect a set of intermediate parameters (which will be called the model parameters) in the calculation of the response.

In the present paper we consider design of microwave circuits with the following concepts treated as an integral part of the design process: optimal design centering, optimal design tolerancing, optimal design tuning, parasitic effects, uncertainties in the circuit modeling, and mismatches at the source and the load.

Manuscript received November 14, 1975; revised March 15, 1976. This work was supported by the National Research Council of Canada under Grant A7239 and by a Graduate Fellowship of the Rotary Foundation to one of the authors (H.T.). This paper is based on material presented at the 1975 IEEE International Microwave Symposium, Palo Alto, CA, May 12–14, 1975.
J. W. Bandler is with the Group on Simulation, Optimization, and Control and the Department of Electrical Engineering, McMaster University, Hamilton, Ont., Canada.
P. C. Liu was with the Group on Simulation, Optimization, and Control and the Department of Electrical Engineering, McMaster University, Hamilton, Ont., Canada. He is now with Bell-Northern Research, Verdun, P.Q., Canada.
H. Tromp was with the Group on Simulation, Optimization, and Control and the Department of Electrical Engineering, McMaster University, Hamilton, Ont., Canada. He is now with the Laboratory of Electromagnetism and Acoustics, University of Ghent, Ghent, Belgium.

II. Theory

The Tolerance-Tuning Problem

In this section we introduce some of the notation and briefly review the parameters involved in the tolerance-tuning problem.

We consider first a vector of nominal design parameters $\boldsymbol{\phi}^0$ and a corresponding vector containing the manufacturing tolerances $\boldsymbol{\varepsilon}$. Thus, for k variables,

$$\boldsymbol{\phi}^0 \triangleq \begin{bmatrix} \phi_1^0 \\ \phi_2^0 \\ \vdots \\ \phi_k^0 \end{bmatrix} \qquad \boldsymbol{\varepsilon} \triangleq \begin{bmatrix} \varepsilon_1 \\ \varepsilon_2 \\ \vdots \\ \varepsilon_k \end{bmatrix}. \tag{1}$$

A possible outcome of a design is then

$$\boldsymbol{\phi} = \boldsymbol{\phi}^0 + \boldsymbol{E}\boldsymbol{\mu}_\varepsilon \tag{2}$$

where

$$\boldsymbol{\mu}_\varepsilon \triangleq \begin{bmatrix} \mu_{\varepsilon_1} \\ \mu_{\varepsilon_2} \\ \vdots \\ \mu_{\varepsilon_k} \end{bmatrix} \tag{3}$$

and

$$\boldsymbol{E} \triangleq \begin{bmatrix} \varepsilon_1 & & & \\ & \varepsilon_2 & & \\ & & \ddots & \\ & & & \varepsilon_k \end{bmatrix}. \tag{4}$$

The vector $\boldsymbol{\mu}_\varepsilon$ determines the actual outcome and can, for example, be bounded by

$$-1 \le \mu_{\varepsilon_i} \le 1, \qquad i = 1,2,\cdots,k. \tag{5}$$

It is assumed that the designer has no control over $\boldsymbol{\mu}_\varepsilon$. This leads to the concept of the tolerance region R_ε, namely, the set of points $\boldsymbol{\phi}$ of (2) subject to, for example, (5). An untuned design implies $\boldsymbol{\phi}$ as given by (2). Consider a vector $\boldsymbol{t}$ containing tuning variables corresponding to (1). Thus

$$\boldsymbol{t} \triangleq \begin{bmatrix} t_1 \\ t_2 \\ \vdots \\ t_k \end{bmatrix}. \tag{6}$$

A design outcome with tuning implies

$$\boldsymbol{\phi} = \boldsymbol{\phi}^0 + \boldsymbol{E}\boldsymbol{\mu}_\varepsilon + \boldsymbol{T}\boldsymbol{\mu}_t \tag{7}$$

where

$$\boldsymbol{\mu}_t \triangleq \begin{bmatrix} \mu_{t_1} \\ \mu_{t_2} \\ \vdots \\ \mu_{t_k} \end{bmatrix} \tag{8}$$

and

$$\boldsymbol{T} \triangleq \begin{bmatrix} t_1 & & & \\ & t_2 & & \\ & & \ddots & \\ & & & t_k \end{bmatrix}. \tag{9}$$

The vector $\boldsymbol{\mu}_t$ determines the setting of the tuning elements and we consider, for convenience,

$$-1 \le \mu_{t_i} \le 1, \qquad i = 1,2,\cdots,k. \tag{10}$$

Hence, we have a tuning region R_t centered at $\boldsymbol{\phi}^0 + \boldsymbol{E}\boldsymbol{\mu}_\varepsilon$ for each outcome $\boldsymbol{\mu}_\varepsilon$.

The worst case tolerance-tuning problem is to obtain an optimal set $\{\boldsymbol{\phi}^0,\boldsymbol{\varepsilon},\boldsymbol{t}\}$ such that all possible outcomes (controlled by $\boldsymbol{\mu}_\varepsilon$) can be tuned so as to satisfy the design specifications (by adjusting $\boldsymbol{\mu}_t$) if tuning is available. If tuning is not available all outcomes must satisfy the design specifications. A detailed discussion has been presented [4].

Model Uncertainties

Taking $\boldsymbol{\phi}$ as the vector of physical design parameters which have to be determined and appear in the cost function, we may consider an n-dimensional vector $\boldsymbol{p}$ containing the model parameters, e.g., the parameters appearing in an electrical equivalent circuit. In general, $n \neq k$. We have an associated vector of nominal model parameters $\boldsymbol{p}^0$ and a vector of model uncertainties $\boldsymbol{\delta}$, where

$$\boldsymbol{p}^0 \triangleq \begin{bmatrix} p_1^0 \\ p_2^0 \\ \vdots \\ p_n^0 \end{bmatrix} \qquad \boldsymbol{\delta} \triangleq \begin{bmatrix} \delta_1 \\ \delta_2 \\ \vdots \\ \delta_n \end{bmatrix}. \tag{11}$$

A possible model can then be described by

$$\boldsymbol{p} = \boldsymbol{p}^0 + \boldsymbol{\Delta}\boldsymbol{\mu}_\delta \tag{12}$$

where

$$\boldsymbol{\mu}_\delta \triangleq \begin{bmatrix} \mu_{\delta_1} \\ \mu_{\delta_2} \\ \vdots \\ \mu_{\delta_n} \end{bmatrix} \tag{13}$$

and

$$\boldsymbol{\Delta} \triangleq \begin{bmatrix} \delta_1 & & & \\ & \delta_2 & & \\ & & \ddots & \\ & & & \delta_n \end{bmatrix}. \tag{14}$$

Thus $\boldsymbol{\mu}_\delta$ determines the particular model under consideration. We will assume

$$-1 \le \mu_{\delta_i} \le 1, \qquad i = 1,2,\cdots,n \tag{15}$$

and also the functional dependence on $\boldsymbol{\phi}$ implied by

$$\boldsymbol{p} = \boldsymbol{p}^0(\boldsymbol{\phi}) + \boldsymbol{\Delta}(\boldsymbol{\phi})\boldsymbol{\mu}_\delta. \tag{16}$$

Given a tolerance region in the $\boldsymbol{\phi}$ space it would be hard, in general, to envisage its effect in the $\boldsymbol{p}$ space, even if $\boldsymbol{\delta} = \boldsymbol{0}$. The selection of worst case $\boldsymbol{p}$ is complicated by the modeling uncertainties. Especially when $n < k$ more than one $\{\boldsymbol{\mu}_\varepsilon,\boldsymbol{\mu}_\delta\}$ may give the same worst case $\boldsymbol{p}$. In selecting candidates we will assume, intuitively, that the following is sufficient:

$$\mu_{\varepsilon_i},\mu_{\delta_j} = \pm 1, \qquad i = 1,2,\cdots,k, \quad j = 1,2,\cdots,n. \tag{17}$$

Mismatch Considerations

We consider environmental influences in the form of mismatches at the source and load. The situation is depicted in Fig. 1. The discussion is directed towards handling terminations with prescribed maximum reflection-coefficient amplitudes and arbitrary reference planes, the

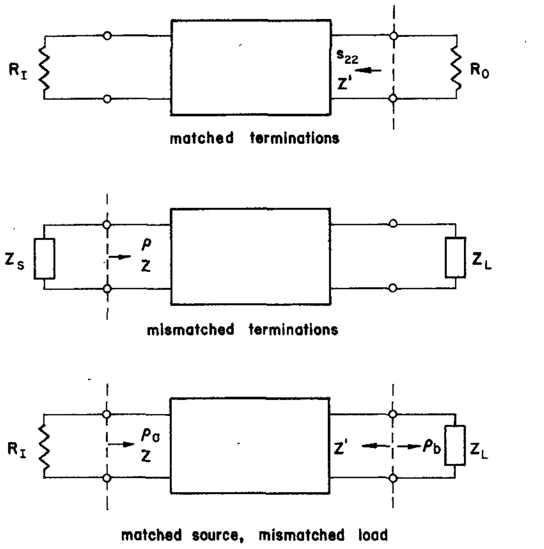

Fig. 1. Two-port circuit viewed with respect to three sets of terminations for defining impedances Z and Z' and reflection coefficients ρ, ρ_a, ρ_b, and s_{22}.

mismatches at different frequencies being, pessimistically, taken as independent.

Fig. 1(a) shows the ideal situation of matched resistive terminations R_I and R_0. Assume that the actual complex terminations as seen by the circuit are Z_S and Z_L, as shown in Fig. 1(b). Then the reflection coefficient

$$\rho_S = \frac{Z_S - R_I}{Z_S + R_I} \tag{18}$$

at the source, and

$$\rho_L = \frac{Z_L - R_0}{Z_L + R_0} \tag{19}$$

at the load. The actual reflection coefficient ρ at the source is given by

$$\rho = \frac{Z - Z_S^*}{Z + Z_S} \tag{20}$$

using the notation of Fig. 1(b). The asterisk denotes the complex conjugate.

Consider the situation depicted in Fig. 1(c). We have, for a matched source and mismatched load, the input impedance Z with the reflection coefficients

$$\rho_a = \frac{Z - R_I}{Z + R_I} \tag{21}$$

and

$$\rho_b = \frac{Z_L - Z'^*}{Z_L + Z'} \tag{22}$$

where Z' is the impedance at the output when the input is matched. Associated with the latter situation is the parameter s_{22} given by [Fig. 1(a)]

$$s_{22} = \frac{Z' - R_0}{Z' + R_0}. \tag{23}$$

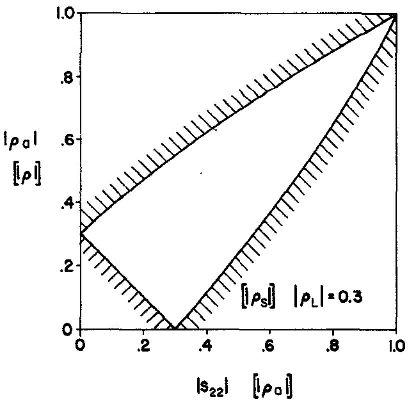

Fig. 2. Feasible region of reflection coefficients given that $|\rho_S| = |\rho_L| = 0.3$.

From (18), (20), and (21) we can obtain ρ in terms of ρ_S and ρ_a. Similarly, from (19), (22), and (23) we can obtain ρ_b in terms of s_{22} and ρ_L. Using Carlin and Giordano [5] we may readily derive the following expressions. For all possible phases

$$\frac{||\rho_a| - |\rho_S||}{1 - |\rho_a||\rho_S|} \le |\rho| \le \frac{|\rho_a| + |\rho_S|}{1 + |\rho_a||\rho_S|} \tag{24}$$

where, assuming a lossless circuit, $|\rho_a| = |\rho_b|$ and

$$\frac{||\rho_L| - |s_{22}||}{1 - |\rho_L||s_{22}|} \le |\rho_b| \le \frac{|\rho_L| + |s_{22}|}{1 + |\rho_L||s_{22}|}. \tag{25}$$

A particular example showing the extreme values of $|\rho_a|$ and $|\rho|$ is shown in Fig. 2.

Explicit upper and lower bounds on $|\rho|$ may be derived. Simplest is the upper bound, given for all possible phases of ρ_S and ρ_L and constant amplitude by

$$\max|\rho| = \frac{K_p + |s_{22}|}{1 + K_p|s_{22}|} \tag{26}$$

where

$$K_p = \frac{|\rho_L| + |\rho_S|}{1 + |\rho_L||\rho_S|}. \tag{27}$$

Let

$$K_q = \frac{|\rho_L| - |\rho_S|}{1 - |\rho_L||\rho_S|} \tag{28}$$

and

$$K_r = -K_q. \tag{29}$$

Assuming all possible phases of ρ_S and ρ_L, but constant amplitude as before, we obtain the following lower bounds.

$$\min|\rho| = \begin{cases} \dfrac{|s_{22}| - K_p}{1 - K_p|s_{22}|}, & \text{if } K_p < |s_{22}| \\ \dfrac{K_q - |s_{22}|}{1 - K_q|s_{22}|}, & \text{if } K_p > |s_{22}|,\ |\rho_L| > |\rho_S|,\ K_q > |s_{22}| \\ \dfrac{K_r - |s_{22}|}{1 - K_r|s_{22}|}, & \text{if } K_p > |s_{22}|,\ |\rho_L| < |\rho_S|,\ K_r > |s_{22}| \\ 0, & \text{otherwise.} \end{cases} \tag{30}$$

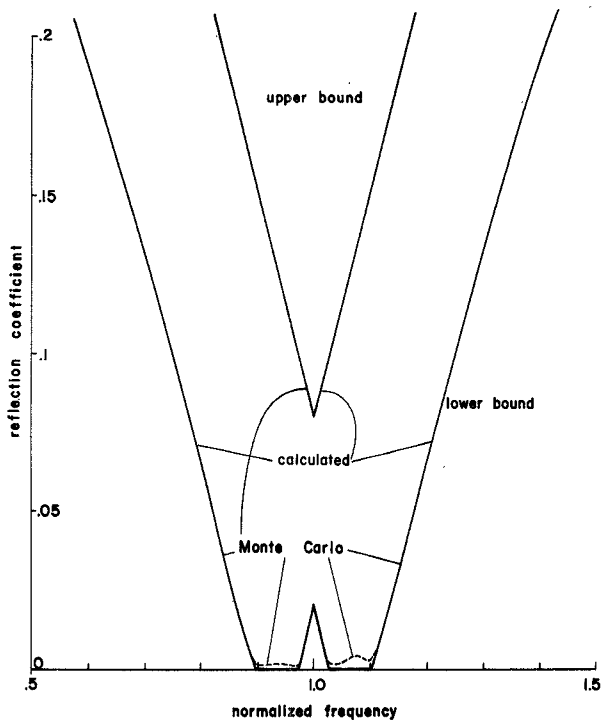

Fig. 3. Upper and lower bounds on reflection coefficient calculated from (26) and (30) and checked by a Monte Carlo analysis (1000 points) for an ideal one-section transformer from 50 to 20 Ω with $|\rho_S| = 0.05$ and $|\rho_L| = 0.03$.

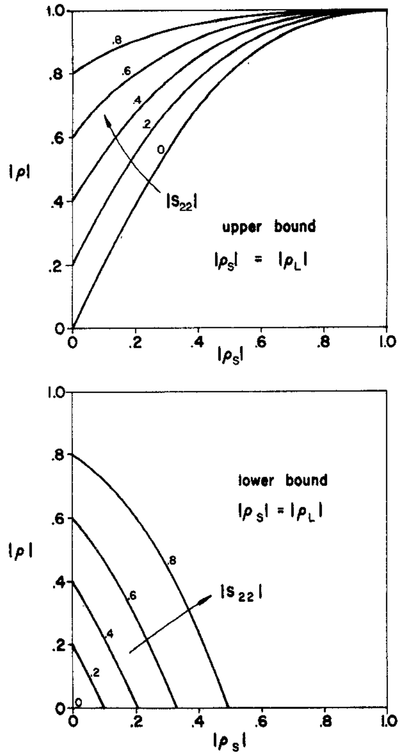

Fig. 4. Upper and lower bounds on $|\rho|$ for $|\rho_S| = |\rho_L|$.

Fig. 3 shows a comparison of these relations with the results of a Monte Carlo analysis with 1000 uniformly distributed values for the phases of ρ_S and ρ_L on $[0,2\pi]$ for a particular example of an ideal one-section transformer from 50 to 20 Ω with $|\rho_S| = 0.05$ and $|\rho_L| = 0.03$.

Assume now all possible amplitudes up to $|\rho_S|$ and $|\rho_L|$ in addition to all possible phases. The upper bound remains the same as (26) but the lower bound becomes

$$\min |\rho| = \begin{cases} \dfrac{|s_{22}| - K_p}{1 - K_p|s_{22}|}, & \text{if } K_p < |s_{22}| \\ 0, & \text{if } K_p \geq |s_{22}|. \end{cases} \tag{31}$$

An illustration for $|\rho_S| = |\rho_L|$ is shown in Fig. 4. We note that under this restriction, the results are not affected by whether all possible amplitudes are considered or not.

Design Specifications

Let all the performance specifications and constraints be expressed in the form

$$g_i \geq 0 \tag{32}$$

where g_i is, in general, an ith nonlinear function of $\boldsymbol{p}(\boldsymbol{\phi})$. Thus we may consider mismatches by an expression of the form

$$g_i = g_i^0(\boldsymbol{p}) + \mu_{\rho_i}(\boldsymbol{p},\rho_{S_i},\rho_{L_i}) \tag{33}$$

where subscript i may denote a sample point and where ρ_S represents the source mismatch and ρ_L the load mismatch. The function μ_{ρ_i} has the effect of shifting the constraint.

Given mismatches, model uncertainties, and so on, obviously influence the nominal design parameters and manufacturing tolerances. An objective, for example, is to find an optimal set $\{\boldsymbol{\phi}^0,\boldsymbol{\varepsilon},\boldsymbol{t}\}$ such that all possible outcomes (controlled by $\boldsymbol{\mu}_\varepsilon$), all possible models (controlled by $\boldsymbol{\mu}_\delta$), and all possible mismatches (controlled by $\boldsymbol{\mu}_\rho$) are accommodated in satisfying the design specifications.

III. Examples

To illustrate some of the ideas presented, we consider two simple circuits. The first includes tuning, the second considers possible model uncertainties, parasitic effects, and mismatched terminations.

Two-Section Transformer

An upper specified reflection coefficient of 0.55 for a two-section lossless transmission-line transformer with quarter-wave-length sections and an impedance ratio of 10:1 was considered at 11 uniformly spaced frequencies on 100-percent relative bandwidth.

Table I shows some results of minimizing certain objective (cost) functions of relative tolerances and tuning ranges. The functions are chosen to penalize small tolerances and large tuning ranges. The design parameters are the normalized characteristic impedances of the two sections, namely, Z_1 and Z_2. The problem has already been considered from the purely tolerance point of view [3]. The parameter ε_i' is the effective tolerance [4] of the ith parameter, i.e.,

$$\varepsilon_i' \triangleq \varepsilon_i - t_i \quad \text{for} \quad \varepsilon_i > t_i. \tag{34}$$

TABLE I
TWO-SECTION 10:1 QUARTER-WAVE TRANSFORMER DESIGN CENTERING, TOLERANCING, AND TUNING

Cost Function*	C_1	C_1	C_1	C_2	C_3	C_4	C_5
Z_1^0	2.1487	2.0340	2.2754	2.5025	1.8748	2.1487	2.1487
Z_2^0	4.7307	4.5355	4.9467	5.3337	4.2642	4.7307	4.7307
ϵ_1/Z_1^0 x 100%	12.74	17.83	17.60	25.08	31.62	31.62	12.74
ϵ_2/Z_2^0 x 100%	12.74	17.60	17.83	31.62	25.08	31.62	12.74
t_1/Z_1^0 x 100%	-	10.00	-	-	31.62	18.88	0.00
t_2/Z_2^0 x 100%	-	-	10.00	31.62	-	18.88	0.00
ϵ_1'/Z_1^0 x 100%	-	7.83	-	-	0.00	12.74	12.74
ϵ_2'/Z_2^0 x 100%	-	-	7.83	0.00	-	12.74	12.74

$*C_1 = Z_1^0/\epsilon_1 + Z_2^0/\epsilon_2$

$C_2 = Z_1^0/\epsilon_1 + Z_2^0/\epsilon_2 + 10(t_2/Z_2^0)$

$C_3 = Z_1^0/\epsilon_1 + Z_2^0/\epsilon_2 + 10(t_1/Z_1^0)$

$C_4 = Z_1^0/\epsilon_1 + Z_2^0/\epsilon_2 + 10(t_1/Z_1^0 + t_2/Z_2^0)$

$C_5 = Z_1^0/\epsilon_1 + Z_2^0/\epsilon_2 + 500(t_1/Z_1^0 + t_2/Z_2^0)$

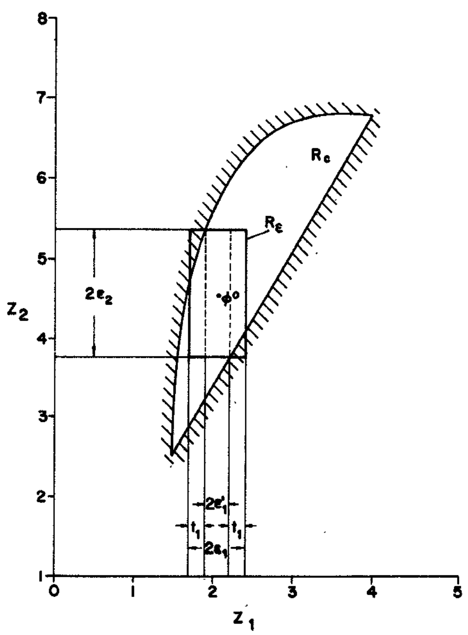

Fig. 5. Optimal solution corresponding to Column 3 of Table I. R_c is the constraint region, i.e., the region for which $|\rho| \leq 0.55$.

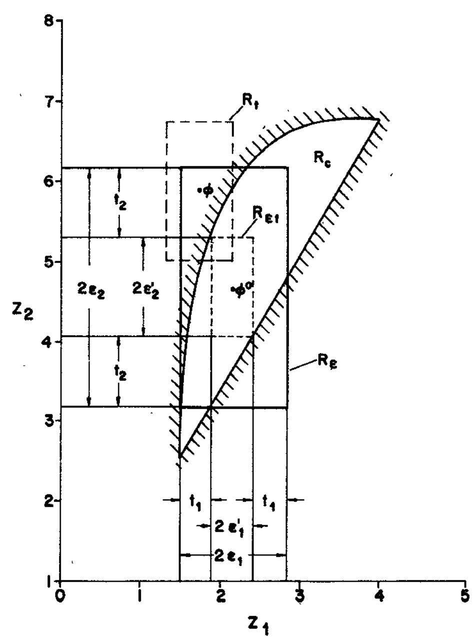

Fig. 6. Optimal solution corresponding to Column 7 of Table I. $R_{\epsilon t}$ is the *effective* tolerance region.

A number of interesting, but not unexpected, features may be noted. Column 2 of Table I shows results for no tuning [3]. Columns 3 and 4 show results when Z_1 and Z_2 are tunable, respectively, by 10 percent. Note that the nominal points move and the tolerances increase. Fig. 5 illustrates the optimal solution corresponding to Column 3. The remaining results indicate solutions when the tuning ranges are variables and included in the objective functions. Observe that the results in the final two columns are essentially the same as those in Column 2. The last column shows how the tuning ranges are automatically set to 0 when they are heavily weighted in the cost function, i.e., they are assumed to be expensive. Fig. 6 corresponds to the situation of Column 7.

Tuning of any component enhances all the tolerances, as expected. Furthermore, if tuning is expensive, it is rejected by the general formulation, which is useful if the designer has a number of possible alternative tunable components and is not sure which components should be effectively tuned ($t_i \geq \epsilon_i$) and which should be effectively toleranced.

One-Section Stripline Transformer

A more realistic example of a one-section transformer on stripline from 50 to 20 Ω is now considered. The physical

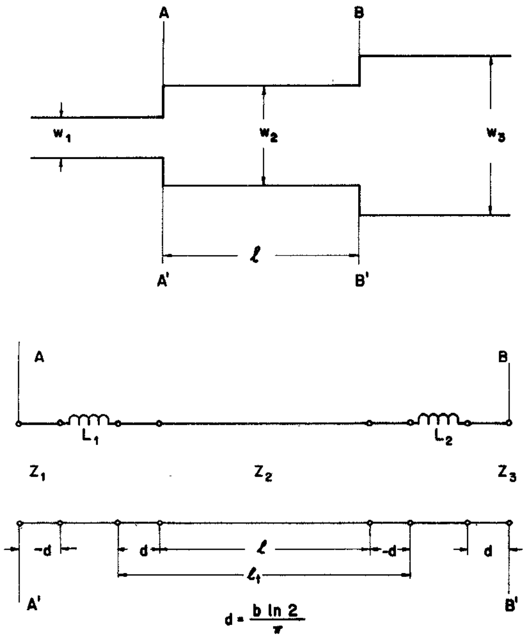

Fig. 7. Stripline transformer and equivalent circuit.

circuit and its equivalent are depicted in Fig. 7. The specifications are listed in Table II. Also shown are source and load mismatches to be accounted for as well as fixed tolerances on certain fixed nominal parameters and assumed uncertainties in model parameters.

Thirteen physical parameters implying 2^{13} extreme points are

$$\phi = \begin{bmatrix} w_1 \\ w_2 \\ w_3 \\ l \\ \sqrt{\varepsilon_{r1}} \\ \sqrt{\varepsilon_{r2}} \\ \sqrt{\varepsilon_{r3}} \\ b_1 \\ b_2 \\ b_3 \\ t_{s1} \\ t_{s2} \\ t_{s3} \end{bmatrix} \begin{matrix} \left.\begin{matrix} \\ \\ \\ \\ \end{matrix}\right\} \text{variable nominal and variable tolerances} \\ \left.\begin{matrix} \\ \\ \\ \\ \\ \\ \\ \\ \\ \end{matrix}\right\} \text{fixed nominal and fixed tolerances} \end{matrix} \tag{35}$$

where w denotes strip width, l the length of the middle section, ε_r the dielectric constant, t_s the strip thickness, and b the substrate thickness. Tolerances on ε_r, b, and t_s were imposed independently for the three lines allowing independent outcomes. Nominal values for corresponding parameters were the same throughout.

Six model parameters implying 2^6 extreme points are

$$p = \begin{bmatrix} D_1 \\ D_2 \\ D_3 \\ L_1 \\ L_2 \\ l_t \end{bmatrix} \tag{36}$$

where D denotes effective linewidth, L the junction parasitic inductance, and l_t the effective section length.

TABLE II
ONE-SECTION STRIPLINE TRANSFORMER

Center Frequency	5 GHz
Frequency Band	4.5 - 5.5 GHz
Reflection Coefficient Specification	0.25 (upper)
Source Impedance	50 Ω (nominal)
Load Impedance	20 Ω (nominal)
Source Mismatch (Maximum)	0.025 (reflection coeff.)
Load Mismatch (Maximum)	0.025 (reflection coeff.)
ε_r	2.54 ± 1%
b	6.35 mm ± 1%
t_s	0.051 mm ± 5%
Uncertainty on L_1, L_2	3%
D_1, D_2, D_3	1%
ℓ_t	1 mm

The formula for D_i used is [6]

$$D_i = w_i + \frac{2b_i}{\pi} \ln 2 + \frac{t_{si}}{\pi}\left[1 - \ln \frac{2t_{si}}{b_i}\right], \qquad i = 1,2,3. \tag{37}$$

The formula is claimed to be good for $w_i/b_i > 0.5$. A 1-percent uncertainty was rather arbitrarily chosen for D_i. The characteristic impedance Z_i is then found as

$$Z_i = \frac{30\pi(b_i - t_{si})}{D_i\sqrt{\varepsilon_{ri}}}. \tag{38}$$

The values of L_i were calculated as [7]

$$L_i = \frac{30\bar{b}_i}{c} K_i, \qquad i = 1,2 \tag{39}$$

where c is the velocity of light *in vacuo* and

$$K_i = \ln\left[\left(\frac{1-\alpha_i^2}{4\alpha_i}\right)\left(\frac{1+\alpha_i}{1-\alpha_i}\right)^{\{[\alpha_i + (1/\alpha_i)]/2\}}\right] + \frac{2}{A_i}$$

$$\alpha_i = \frac{D_i}{D_{i+1}} < 1$$

$$A_i = \left(\frac{1+\alpha_i}{1-\alpha_i}\right)^{2\alpha_i} \frac{1+S_i}{1-S_i} - \frac{1+3\alpha_i^2}{1-\alpha_i^2}$$

$$S_i = \sqrt{1 - \frac{D_{i+1}^2}{\bar{\lambda}_{gi}^{\,2}}}$$

$$\bar{\lambda}_{gi} = \frac{c}{f\sqrt{\bar{\varepsilon}_{ri}}}$$

$$\bar{b}_i = 0.5(b_i + b_{i+1})$$

$$\sqrt{\bar{\varepsilon}_{ri}} = 0.5(\sqrt{\varepsilon_{ri}} + \sqrt{\varepsilon_{r(i+1)}}).$$

Mean values across the junctions of adjacent sections of $\sqrt{\varepsilon_r}$ and b are taken since actual values in our model can be different across junctions. Data for estimating the

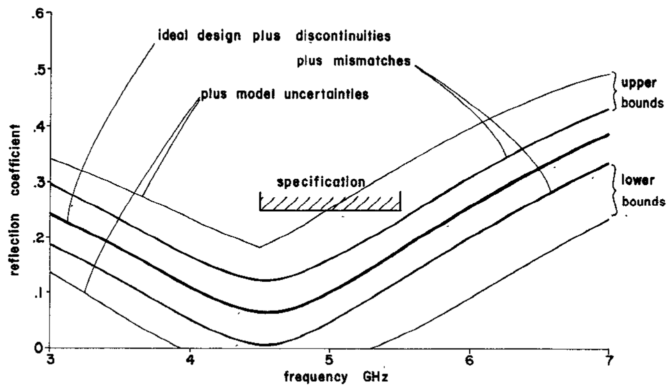

Fig. 8. Worst case analyses for the stripline transformer. Note that physical parameter tolerances are not included.

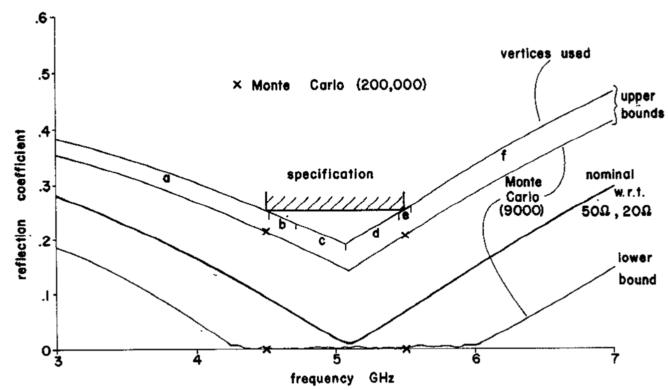

Fig. 9. Final results for the stripline transformer. The letters $a, b, \cdots, f$ indicate different vertices (designs) determining the worst case in different frequency bands.

uncertainties on L_i are available [6], [7]. Other approximations have, however, been introduced due to the tolerancing. A 3-percent uncertainty on L_i was adopted.

The length l_t is nominally the same as l. Experimental results [6] indicate possibly large inaccuracies in d (see Fig. 7) and that it depends at least on α, so that it is actually different for the two junctions. A rather pessimistic estimated error of 1 mm on l_t was chosen.

Maximum mismatch reflection coefficients of 0.025 were chosen for the source and load. Note that these values are assumed with respect to 50 and 20 Ω, respectively. The relevant formulas developed in Section II cannot be applied directly, since Z_1 and Z_3, which are affected by tolerances, must be considered for normalization. We take, most pessimistically,

$$|\rho_S| = \frac{0.025 + |\rho_1|}{1 + 0.025|\rho_1|} \tag{40}$$

where

$$\rho_1 = \frac{50 - Z_1}{50 + Z_1}$$

and

$$|\rho_L| = \frac{0.025 + |\rho_3|}{1 + 0.025|\rho_3|} \tag{41}$$

where

$$\rho_3 = \frac{20 - Z_3}{20 + Z_3}.$$

Fig. 8 summarizes some of the results obtained from worst case analyses. Depicted are curves of the ideal design with discontinuity (parasitic) effects taken into account; upper and lower bounds on the response with source and load mismatches also added; finally, upper and lower responses with model uncertainties further deteriorating the situation.

A worst case study was made to select a reasonable number of constraints from the possible $2^{19} = 2^{13} \times 2^6$, since 2^{19} would have required about 5000 s of CDC 6400 computing time per frequency point. The vertex selection

TABLE III
RESULTS FOR ONE-SECTION STRIPLINE TRANSFORMER

Cost Function	$\frac{1}{100}\left(\frac{w_1^0}{\varepsilon_{w_1}}+\frac{w_2^0}{\varepsilon_{w_2}}+\frac{w_3^0}{\varepsilon_{w_3}}+\frac{\ell^0}{\varepsilon_\ell}\right)$		
Sample Points	4.5, 5.5		GHz
Number of Variables	8		
State of Solution	Intermediate	Final	
Number of Final Constraints	18	21	
Number of Optimizations	7	9	
CDC 6400 Time	2	4	min
Minimal Cost	4.82	4.93	
w_1^0	4.660	4.642	mm
w_2^0	8.968	8.910	mm
w_3^0	15.463	15.442	mm
ℓ^0	8.494	8.437	mm
$\varepsilon_{w_1}/w_1^0 \times 100$	0.94	0.92	%
$\varepsilon_{w_2}/w_2^0 \times 100$	1.20	1.13	%
$\varepsilon_{w_3}/w_3^0 \times 100$	0.74	0.70	%
$\varepsilon_\ell/\ell^0 \times 100$	0.64	0.65	%

procedure for the 13 physical parameters follows Bandler *et al.* [3]. From each of the selected vertices the worst values of the modeling parameters are chosen. Only the band edges are used during optimization. After each optimization the selection procedure is repeated, new constraints being added, if necessary.

Results on centering and tolerancing using DISOPT [8] are shown in Table III. The final number of constraints used is 21 after 9 optimizations required to identify the final constraints. Less than 4 min on the CDC 6400 was altogether required. (An intermediate, less accurate, solution is obtained using 18 constraints after 7 optimizations requiring 2 min on the CDC 6400.) To verify that the solution meets the specification, the constraint selection procedure was repeated at 21 points in the band.

Fig. 9 presents final results for this example. The reason for the discrepancy between the worst cases when vertices are used and when the Monte Carlo analysis is used is that the Monte Carlo analysis does not employ the pessimistic approximations of (40) and (41).

IV. Conclusions

The concepts we have described and the results obtained are promising. Our approach is the most direct way of currently obtaining minimum cost designs under practical situations, at least in the worst case sense. It is felt that this work is a significant advance in the art of computer-aided design, since the approach permits the inclusion of all realistic degrees of freedom of a design and all physical phenomena that influence the subsequent performance.

The approach automatically creates a tradeoff between physical tolerances (implying the cost of the network), model parameter uncertainties (implying our knowledge of the network), the quality of the terminations, and, eventually, the cost of tuning. Our approach to mismatches permits input and output connecting lines of arbitrary length—an important step towards modular design.

The conventional computer-aided design process, which seeks a single nominal design or its extension which attempts to find a design center influenced by sensitivities (see, for example, Rauscher and Epprecht [9]), would normally be a preliminary investigation to find a starting point for the work we have in mind.

References

[1] J. W. Bandler, "Computer optimization of inhomogeneous waveguide transformers," *IEEE Trans. Microwave Theory Tech.*, vol. MTT-17, pp. 563–571, Aug. 1969.
[2] H. Tromp and G. Hoffman, "Computer optimization of 3 dB microstrip hybrids taking into account dispersive, coupling and junction effects," *Proc. 1973 European Microwave Conf.* (Brussels, Belgium, Sept. 1973), Paper A.12.4.
[3] J. W. Bandler, P. C. Liu, and J. H. K. Chen, "Worst case network tolerance optimization," *IEEE Trans. Microwave Theory Tech.*, vol. MTT-23, pp. 630–641, Aug. 1975.
[4] J. W. Bandler, P. C. Liu, and H. Tromp, "A nonlinear programming approach to optimal design centering, tolerancing and tuning," *IEEE Trans. Circuits and Systems*, vol. CAS-23, pp. 155–165, March 1976.
[5] H. J. Carlin and A. B. Giordano, *Network Theory*. Englewood Cliffs, N.J.: Prentice-Hall, 1964, pp. 331–334.
[6] H. M. Altschuler and A. A. Oliner, "Discontinuities in the center conductor of symmetric strip transmission line," *IRE Trans. Microwave Theory Tech.*, vol. MTT-8, pp. 328–339, May 1960.
[7] V. Nalbandian and W. Steenaart, "Discontinuities in symmetric striplines due to impedance steps and their compensations," *IEEE Trans. Microwave Theory Tech.*, vol. MTT-20, pp. 573–578, Sept. 1972.
[8] J. W. Bandler and J. H. K. Chen, "DISOPT—A general program for continuous and discrete nonlinear programming problems," *Int. J. Systems Science*, vol. 6, pp. 665–680, 1975.
[9] C. Rauscher and G. Epprecht, "Simplified approach to sensitivity optimization by use of scattering parameters," in *Proc. 1974 European Microwave Conf.* (Montreux, Switzerland, Sept. 1974), pp. 394–398.

Effect of the Magnetic Perturbation on Magnetostatic Surface-Wave Propagation

MAKOTO TSUTSUMI, MEMBER, IEEE, TUSHAR BHATTACHARYYA, AND NOBUAKI KUMAGAI, SENIOR MEMBER, IEEE

***Abstract*—This paper discusses the propagation of the magnetostatic surface wave in two ferrite slabs (namely, YIG and Ga-YIG) with different magnetic saturations, and considers a weak coupling in between them. The theoretical results are obtained by using the conventional perturbation technique which is subsequently supported by experiment. Further, the time delay in group velocity affected by the magnetic perturbation is treated theoretically.**

Manuscript received November 19, 1975; revised March 1, 1976. T. Bhattacharyya received financial assistance from Matsushita Research Institute, Tokyo, Japan, to carry out this research.

M. Tsutsumi and N. Kumagai are with the Department of Electrical Communication Engineering, Osaka University, Yamada Kami, Osaka 565, Japan.

T. Bhattacharyya is with the Department of Electrical Communication Engineering, Osaka University, Yamada Kami, Osaka 565, Japan, on leave from Jadavpur University, Calcutta 32, India.

I. Introduction

The propagation loss associated with a magnetostatic surface wave on a YIG slab is relatively low [1]. Recently, a millimeter delay-line equalizer has been reported as one of the applications of these surface waves [2].

Since surface waves tend to concentrate the major part of their energy near the surface [3], this phenomenon can be utilized to couple the wave to other circuits through the surface to manipulate the propagation characteristic through this coupling. In particular, one problem that arises is the control of the propagation characteristic by changing the distance between the two interacting slabs. This type of problem has already been considered by